J. Physiol. (1985), **362**, *pp.* 107–130
With 12 text-figures
Printed in Great Britain

CALCIUM-DEPENDENT INWARD CURRENT IN *APLYSIA* BURSTING PACE-MAKER NEURONES

BY RICHARD H. KRAMER* AND ROBERT S. ZUCKER

From the Department of Physiology–Anatomy, University of California, Berkeley, CA 94720, U.S.A.

(*Received 30 May 1984*)

SUMMARY

1. Depolarizing voltage-clamp pulses elicit a triphasic series of tail currents (phase I, II and III) in *Aplysia* burst-firing neurones L2–L6. The sequence and time course of the tail currents resemble slow changes in membrane potential which follow bursts in the unclamped cell.

2. The phase II tail current is an inward current with a time course similar to that of the depolarizing after-potential (d.a.p.) which follows bursts in the unclamped cell. The phase II tail current is suppressed by depolarizing pulses which approach E_{Ca}, is blocked by Ca^{2+} current antagonists (Co^{2+} and Mn^{2+}), and is blocked by intracellular injection of EGTA.

3. The phase II tail current is not blocked by agents which block Na^+-dependent action potentials, the Na^+–Ca^{2+} exchange pump, or the Na^+–K^+ exchange pump. The phase II tail current is not blocked by the elimination of large outward K^+ currents which can lead to extracellular K^+ accumulation. Thus, the phase II tail current is not generated by any of these processes.

4. The phase II tail current is reduced by about 60% following substitution of tetramethylammonium (TMA^+) for external Na^+, but is unaffected by reducing external Cl^-.

5. The phase II tail current is distinct from a persistent inward Ca^{2+} current which underlies the negative resistance region of the steady-state current–voltage relation of bursting cells. The persistent inward current is only slightly reduced by TMA^+ substitution for Na^+, and is enhanced by EGTA injection.

6. Injection of Ca^{2+} into *Aplysia* bursting cells elicits a biphasic (inward–outward) current. The inward current can be observed in isolation after blocking the outward component (Ca^{2+}-activated K^+ current) with 50 mM-external tetraethylammonium.

7. The Ca^{2+}-elicited inward current has a reversal potential near -22 mV, and is non-selective for Na^+, K^+ and Ca^{2+}. The reversal potential is unaffected by changes in Cl^- and pH. The Ca^{2+}-activated conductance is apparently voltage independent.

8. We propose that the phase II tail current, and hence the d.a.p., is due to the Ca^{2+}-dependent activation of a voltage-independent non-specific cationic conductance. This conductance participates in generating the depolarizing phase of bursting pace-maker activity.

* Present address and reprint requests: Department of Biochemistry, Brandeis University, Waltham, MA 02254, U.S.A.

INTRODUCTION

Bursting firing patterns due to endogenous oscillations in membrane potential (V_m) have been found in neurones from a number of invertebrate nervous systems (Alving, 1968; Gainer, 1972; Calabrese, 1979; Tazaki & Cooke, 1979; Gola & Selverston, 1981) and recently in mammalian hypothalamic neurones (Gahwiler & Dreifuss, 1979; Andrew & Dudek, 1983). The ionic mechanisms responsible for bursting pace-maker activity have been studied extensively, especially in molluscan neurones, but are still not well understood. The depolarizing phase of bursting activity in these cells is thought to be due to a slow, regenerative inward current. Eckert & Lux (1976) detected a persistent inward current in *Helix* bursting neurones which exhibits slow activation and inactivation kinetics, and which is carried by Ca^{2+}. This current can be observed most clearly during small (about 10 mV) depolarizing voltage-clamp pulses from a holding potential (V_h) within the pace-maker voltage range (i.e. -30 to -50 mV), and is responsible for the region of negative slope resistance observed in the late (steady-state) current–voltage relationship of these cells (Eckert & Lux, 1976). A similar negative resistance region has been found in *Aplysia* bursting pace-maker neurones, and attributed to a slow inward current carried by Ca^{2+} (Gorman, Hermann & Thomas, 1982), Na^+ (Smith, Barker & Gainer, 1975; Carnevale & Wachtel, 1980), or both Ca^{2+} and Na^+ (Johnston, 1976).

Recently, a small, slow inward tail current which follows brief voltage-clamp depolarizations was detected in molluscan bursting neurones (Thompson, 1976; Smith, 1978; Lewis, 1984; Adams, 1985). It has been suggested that this current generates the depolarizing after-potential (d.a.p.) which follows spikes in bursting cells. The inward tail current has a time course similar to that of the d.a.p., and both the tail current and the d.a.p. are reduced when Na^+ or Ca^{2+} are removed from the bathing medium (Thompson, 1976). It has also been suggested that d.a.p.s provide a mechanism for sustaining repetitive firing, and are critical for the depolarizing phase of bursting pace-maker activity (Thompson & Smith, 1976).

We have examined a series of slow tail currents which flow following voltage-clamp depolarizations in *Aplysia* bursting neurones. We present evidence here that the slow inward phase of this tail current is dependent upon the entry of Ca^{2+} during the depolarizing pulse, and is due to the Ca^{2+}-dependent activation of an inward current. Intracellular injection of Ca^{2+} into bursting pace-maker neurones activates an inward current as well as an outward K^+ current, as described previously (Hofmeier & Lux, 1981). We have examined the inward current in isolation, by blocking the Ca^{2+}-activated K^+ current ($I_{K(Ca)}$) (for review see Meech, 1978) with external tetraethylammonium (TEA). The Ca^{2+}-elicited inward current has several characteristics in common with the slow inward tail current. Therefore, we propose that the Ca^{2+}-activated inward current is responsible for both the slow inward tail current and the d.a.p.

METHODS

All experiments were done on the left upper quadrant bursting (l.u.q.b.) neurones L2–L6 (Frazier, Kandel, Kupfermann, Waziri & Coggeshall, 1967) of the abdominal ganglion of *Aplysia californica*. The ganglion was removed from the animal, pinned to the Sylgard base of a plastic chamber filled with artificial seawater (ASW) at 21–23 °C, and the overlying connective tissue sheath was removed. A section of the ganglion containing the l.u.q.b. neurones and some adjoining somata and neuropil was isolated by circumscribing it with a razor blade sliver to within 500 μm of the somata, in order to eliminate spontaneous synaptic currents and uncontrolled axonal spikes in voltage-clamped cells. The calculated length constant of typical *Aplysia* axons is 5–16 mm (Graubard, 1975). Lewis, Evans & Wilson (1984) have found that the axon 300 μm from the soma follows closely the soma potential under voltage clamp. Usually one or two of the l.u.q.b. cells continued to exhibit spontaneous bursting pace-maker activity after axotomy. Cell R15 rarely exhibited spontaneous bursting after axotomy, and was not used for the experiments presented here, except where indicated.

TABLE 1. Composition of artificial sea water (ASW) solutions (mM)

Solution	Na^+	K^+	Ca^{2+}	Mg^{2+}	Cl^-	HEPES	Other
Normal ASW	495	10	10	50	620	10	—
40 mM-K^+	455	40	10	50	620	10	—
1 mM-K^+	504	1	10	50	620	10	—
Low Cl^-	495	10	10	50	130	10	490 $CH_3SO_4^-$
50 mM-TEA^+	495	10	10	50	670	10	50 TEA^+
100 mM-TEA^+	495	10	10	50	720	10	100 TEA^+
0 Ca^{2+}, Co^{2+}	495	10	—	50	620	10	10 Co^{2+}
0 Ca^{2+}, Mn^{2+}	495	10	—	50	620	10	10 Mn^{2+}
0 Na^+, TMA^+	—	10	10	50	620	10	495 TMA^+
0 Na^+, Li^+	—	10	10	50	620	10	495 Li^+
0 Na^+, sucrose	—	10	10	50	125	10	837 sucrose
0 Na^+, 0 Ca^{2+}	—	10	—	60	620	10	495 TMA^+

Bathing solutions used are shown in Table 1. All of these solutions were buffered to pH 7·5 with HEPES (*N*-2-hydroxyethyl piperazine-*N'*-2-ethane sulphonic acid). ASW solutions with pH values of 6·8 and 8·3 were prepared with MOPS (morpholinopropane sulphonic acid) or Tris buffer, respectively, instead of HEPES. In Na^+-free ASW solutions, Na^+ was substituted with an equimolar concentration of tetramethylammonium (TMA^+) or Li^+, or an isosmotic concentration of sucrose. In Ca^{2+}-free ASW solutions, Ca^{2+} was substituted with an equimolar concentration of Co^{2+}, Mn^{2+} or Mg^{2+}. Tetraethylammonium (TEA) (50 or 100 mM) and 4-aminopyridine (8 mM) were added to ASW solutions without osmotic adjustment. Tetrodotoxin (TTX) and ouabain were added directly to the bath. During solution changes, the chambers were perfused with at least 10 bath volumes in 5 min.

In our voltage-clamp arrangement, the transmembrane potential was measured differentially between intracellular and extracellular voltage-recording electrodes, and wide-band negative feed-back current was applied between a second intracellular electrode and an extracellular grounding electrode. The glass intracellular electrodes were filled with 3 M-KCl and were pulled from thin-wall tubing (1·5 mm outside diameter, W–P Instruments) to a resistance of 1–3 MΩ. The extracellular electrodes (Ag–AgCl pellets) were placed in 3 M-KCl in contact with a short ASW–agar bridge to the bath. No compensation was made for the resistance in series with the membrane, r_s, which was about 1 kΩ. The difference between the true and recorded membrane potential ($V_m = I_m r_s$) would have been less than 5 mV during the largest membrane currents (5 μA) elicited by our experimental protocols, except where noted otherwise.

The feed-back amplifier included series capacitance in the feed-back circuit to boost the low-frequency gain. The speed of the voltage clamp was maximized in some experiments by using a wide-band capacitance-compensated electrometer to record from the voltage micro-electrode. Under optimum conditions, capacitive current settled to 1 % of its maximal value within 0·5 ms of command steps.

Small tail currents were recorded with a high-gain current monitor utilizing a one-pole low-pass filter with a time constant of 10 ms. Depending on the initial magnitude and time course of the tail current, up to several hundred milliseconds might be obscured because of saturation of this amplifier. The holding current required to clamp the cell at a given V_m was often more than an order of magnitude greater than the slow tail currents of interest. In order to observe these currents at high gain, a sample-and-hold circuit was used to set the high-gain current monitor output to zero at all hold potentials. The remainder of the recording, stimulating and voltage-clamp circuitry were conventional. Signals were displayed on an oscilloscope and two-channel rectilinear pen recorder and stored on magnetic tape. In some experiments tail current records were digitized for subtraction with the use of a digitizing signal averager (Neurolog NL 750, Medical Systems Corp., Great Neck, NY). The variability among measurements is expressed as mean ± S.E. of the mean.

Ca^{2+} and EGTA (ethylene glycol-bis-(β-aminoethyl ether)-N,N'-tetra-acetic acid) were injected ionophoretically into cells through thin-wall glass micro-electrodes. Ca^{2+}-injection electrodes were filled with 0·5 M-$CaCl_2$. EGTA-injection electrodes were filled with 0·25 M-K_2EGTA. All ions were injected under voltage clamp so that there was no change in the current flowing across the membrane during the injection. Injections were accomplished with a constant current iontophoresis unit (model 160, W–P Instruments), while the current was monitored with an isolation amplifier circuit.

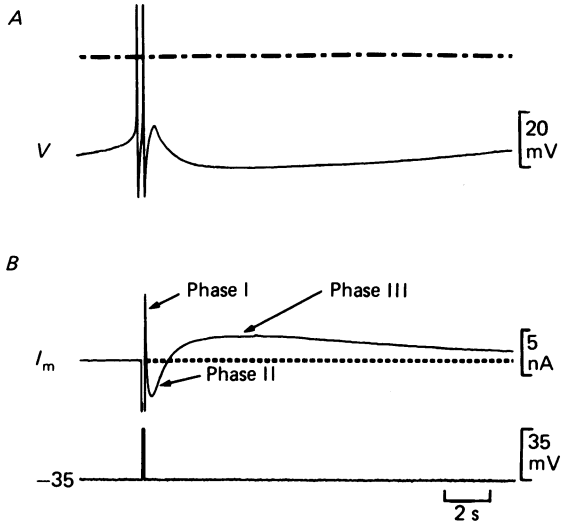

Fig. 1. Slow tail currents in an l.u.q.b. neurone. *A*, one cycle of spontaneous bursting pace-maker activity in an unclamped l.u.q.b. cell. The dashed line denotes the zero potential level. *B*, triphasic series of slow tail current, in the same cell, resulting from a 50 ms depolarizing voltage-clamp pulse to 0 mV from a V_h of −35 mV. Note the close correspondence between the hyperpolarization after the last spike in the burst, the d.a.p., and the inter-burst hyperpolarization in *A* to the tail current phases I, II and III in *B*.

RESULTS

Slow tail currents in bursting neurones

In order to determine the nature of the slow currents which generate the pace-maker cycle of bursting neurones, we investigated the slow tail currents which follow depolarizing voltage-clamp pulses in l.u.q.b. cells. The slow currents which flow after a brief depolarizing pulse are similar in wave form to the slow currents which flow after a spike or a burst of spikes, as previously described in other molluscan bursting neurones (Carnevale & Wachtel, 1980; Lewis, 1984; Adams, 1985). When an l.u.q.b. neurone is given a short pulse (< 100 ms) from a holding potential (V_m) which is near

the unclamped cell's resting potential (−35 to −45 mV) up to a test potential (V_t) of about 0 mV, a series of slow tail currents are observed (Fig. 1*B*). After the pulse, the net tail current is initally outward (phase I), then the net tail current turns inward for up to 1 s (phase II), and finally it is outward again for up to 30 s (phase III). The net tail current at any time after the pulse represents the sum of all the individual ionic currents, at that time, which were activated or inactivated by processes initiated by the pulse, and is measured with respect to the holding current before the pulse.

The series of tail currents resembles changes in voltage which occur at the end of a spontaneous burst of spikes in the unclamped cell (Fig. 1*A*). At the end of the last spike in the burst, there is an after-hyperpolarization, then a d.a.p., and finally a slow inter-burst hyperpolarization during the inter-burst interval. These events correspond closely in sequence and in time course to the tail current phases I, II and III. Since tail current phase II corresponds to the d.a.p., and d.a.p.s contribute to repetitive firing during the depolarizing phase of bursting (Thompson & Smith, 1976), understanding the conductance mechanism which accounts for the phase II current is important for understanding the ionic basis of bursting activity.

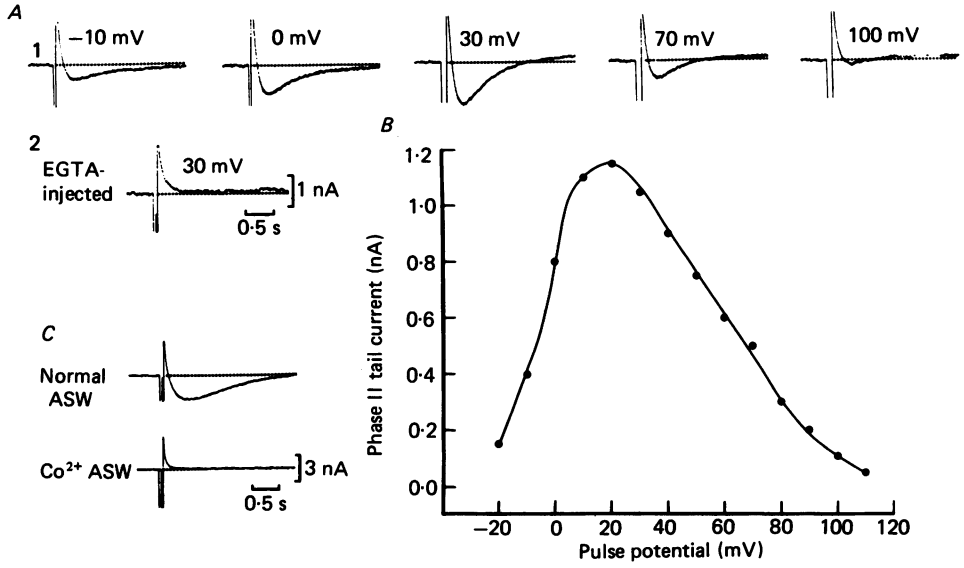

Fig. 2. Ca^{2+} dependence of the phase II tail current. *A*1, phase II tail currents following 10 ms pulses from a V_h of −60 mV to the pulse potential indicated. *A*2, tail current generated in the same cell as in *A*1, after 4 min, 400 nA intracellular injection of EGTA. Pulse as in *A*1 to +30 mV. *B*, relation between pulse potential and the peak amplitude of the phase II tail current. Pulses as in *A*1. *C*, the effect of replacement of external Ca^{2+} with Co^{2+} on the phase II tail current in a different l.u.q.b. cell. Tail currents were elicited by 20 ms pulses to +20 mV from a V_h of −60 mV.

Dependence of phase II tail current on the influx and accumulation of Ca^{2+}

In order to study the tail current component which predominates during phase II in relative isolation from the other tail current components, we usually used brief (< 50 ms) depolarizing pulses from a V_h near −60 mV, which is just above the reversal potential of the phase I tail current (about −65 mV) and near the potential at which the phase III component is nearly completely suppressed (Kramer & Zucker,

1985). Fig. 2*A*1 shows phase II tail currents following 10 ms pulses to various test potentials. The peak inward current is largest following pulses which elicit a maximal Ca^{2+} influx (i.e. +30 mV), and is much smaller following pulses which approach E_{Ca} (probably near +150 mV: Hagiwara & Byerly, 1981), and therefore elicit a minimal Ca^{2+} influx. The relationship between the inward current amplitude during phase II and the pulse potential has an inverted U shape (Fig. 2*B*). In four l.u.q.b. cells, the largest peak phase II tail current occurred at pulse potentials between +20 and +40 mV, and the amplitude of the current elicited by a pulse to +100 mV ranged from 10 to 20% of the largest current. Various neurophysiological processes which require Ca^{2+} influx also display an inverted U-shaped relationship with pulse potential; for example, the activation of $I_{K(Ca)}$ (Meech & Standen, 1975; Gorman & Thomas, 1980*a*), Ca^{2+}-dependent inactivation of Ca^{2+} current (Brehm & Eckert, 1978; Eckert & Tillotson, 1981); and neurotransmitter release at squid central synapses (Katz & Miledi, 1967). Therefore, it seems likely that the inward current which predominates during phase II is Ca^{2+}-activated.

We tested this idea further by examining the phase II current elicited in ASW in which all of the Ca^{2+} was substituted with divalent cations (Co^{2+} or Mn^{2+}) which block Ca^{2+} channels (for review, see Hagiwara & Byerly, 1981). Under these conditions the phase II current usually was reversibly blocked ($n = 7$ cells) (Fig. 2*C*), although occasionally ($n = 2$ cells) it was only reduced by 79–85%. Other Ca^{2+}-dependent processes, such as $I_{K(Ca)}$ (Akaike, Brown, Dahl, Higashi, Isenberg, Tsuda & Yatani, 1983), are often highly resistant to blockage by removal of external Ca^{2+} and replacement with divalent cations such as Co^{2+}, but can be effectively blocked with intracellular EGTA. Likewise, intracellular iontophoresis of EGTA into each of six l.u.q.b. cells eliminated the phase II tail current (Fig. 2*A*2). The remaining outward tail current reversed at −70 mV and was reduced more than 80% by 1 mM-4-aminopyridine, a blocker of the transient K^+ current, I_A (Thompson, 1977).

The nature of the phase II tail current

Effects of tetrodotoxin (TTX). The slow tail currents which follow depolarizing voltage-clamp pulses could result from regenerative voltage changes in poorly clamped regions of axotomized l.u.q.b. neurones, such as the remaining axon stump. In intact l.u.q.b. cells, depolarization of the voltage-clamped cell body elicits delayed, transient inward currents due to action potentials arising in the axon. In addition, patterned bursts of action potential currents (Treistman, 1980) and slow oscillations of the base-line holding current (R. H. Kramer, unpublished observations) sometimes appear in intact l.u.q.b. cells which are voltage-clamped at depolarized V_h (i.e. −25 to −35 mV), indicating that the poorly clamped axon has the intrinsic capability of generating bursting pace-maker activity. It is possible, therefore, that the slow tail currents in axotomized l.u.q.b. cells are due, at least in part, to slow voltage changes in the remaining axon stump. Adams & Levitan (1985) have shown that the phase II tail current of cell R15 can be activated in a nearly all-or-none manner by depolarizing pulses over a narrow voltage range, and can be blocked with hyperpolarizing post-pulses; thus, they have suggested that the phase II tail current in R15 is the result of the passive spread of inward current from a propagating axon spike. Activation of the phase II tail current in l.u.q.b. cells, however, occurs over a wide

range of pulse potentials (Fig. 2), and hyperpolarizing post-pulses produce little change in the phase II current of l.u.q.b. cells (see Fig. 12). Addition of 50 μM-TTX to the ASW, which nearly completely blocks the voltage-dependent Na^+ conductance of action potentials in bursting pace-maker neurones (Adams & Gage, 1979), resulted in a decrease in the phase II tail current amplitude of less than 5 % in three l.u.q.b. cells (Fig. 3*A*). Thus, axonal Na^+ spikes are not necessary for the generation of the phase II tail current in l.u.q.b. cells. The possibility remains, however, that regenerative Ca^{2+}-dependent responses in the axon stump contribute to the slow tail currents.

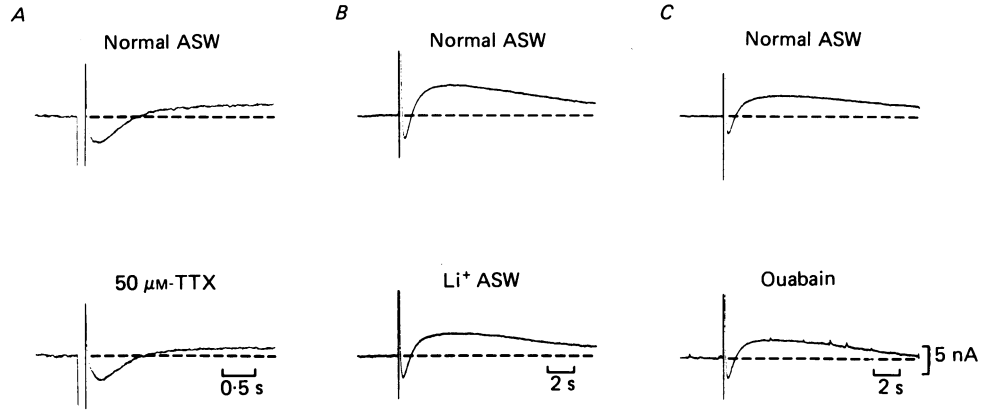

Fig. 3. *A*, effect of 50 μM-TTX on the slow tail current elicited by a 70 ms pulse to 0 mV from a V_h of −55 mV. *B*, effect of equimolar substitution of Li^+ for Na^+ on the tail current elicited by a 50 ms pulse to 0 mV from a V_h of −40 mV. *C*, effect of 0·2 mM-ouabain on the slow tail currents, elicited as in *B*.

Effects of blocking the Na^+–Ca^{2+} exchange pump. The phase II tail current could arise from the activation of an electrogenic Na^+–Ca^{2+} exchange pump (for review see DiPolo & Beaugé, 1983) by the elevated intracellular Ca^{2+} concentration which declines slowly after depolarizing pulses (see, e.g. Gorman & Thomas, 1980*b*; Smith & Zucker, 1980). The Na^+–Ca^{2+} exchange pump is blocked by the replacement of external Na^+ with Li^+ (Blaustein & Hodgkin, 1969). In l.u.q.b. cells, substitution of Li^+ for Na^+ had variable effects on the phase II tail current. In three cells which had been bursting vigorously before being voltage-clamped, Li^+ substitution had only minor effects on the phase II tail current (Fig. 3*B*). In these cells, the effect of Li^+ substitution ranged from an 8 % increase to a 7 % decrease in the peak phase II current elicited at a V_h of −60 mV. In two other possibly less healthy cells, which were not spontaneously bursting before being voltage clamped, Li^+ substitution had a larger effect on the phase II tail current, reducing the peak amplitude by 49 % and 56 %. These results indicate that the activity of the Na^+–Ca^{2+} exchange pump does not directly underlie the phase II tail current, at least in some l.u.q.b. cells. However, activity of the pump may be important for maintaining the conditions under which the phase II tail current can be generated. The operation of the Na^+–Ca^{2+} exchange pump may be involved in removing Ca^{2+} from *Aplysia* neurones (Satin, 1984), especially in cells with a high intracellular Ca^{2+} concentration. It is possible that a

high ambient intracellular Ca^{2+} concentration depresses the processes which lead to activation of the phase II tail current (see Discussion).

Effects of ouabain. The possible involvement of the electrogenic Na^+–K^+ exchange pump in generating the slow tail currents was tested by the addition of ouabain. The slow tail currents in two l.u.q.b. cells were unaffected by the addition of 0·2 mM-ouabain (Fig. 3*C*), although there was an inward shift in the base-line holding current of 10–20 nA, indicating a block of the electrogenic Na^+–K^+ exchange pump.

The phase II current is not due to extracellular K^+ accumulation. Both the d.a.p. and the phase II tail current could result from the accumulation of K^+ in the extracellular space which surrounds the soma. Depolarizing pulses can cause an increase in the external K^+ concentration near molluscan somata (Eaton, 1972; Neher & Lux, 1973; Gorman *et al.* 1982). Bursting cells exhibit a pronounced $I_{K(Ca)}$ (Gorman & Hermann, 1982); therefore, K^+ accumulation and its manifestations may be dependent upon the influx and accumulation of intracellular Ca^{2+}.

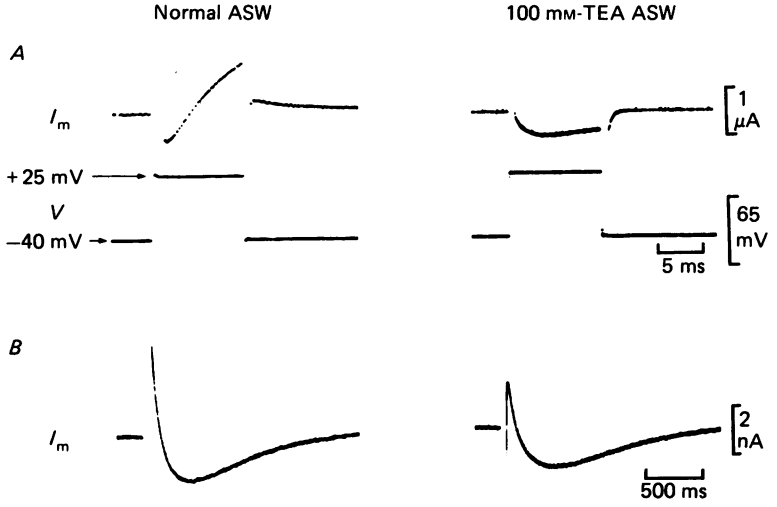

Fig. 4. The phase II tail current is not dependent upon K^+ accumulation outside l.u.q.b. cells. *A*, membrane currents evoked by 15 ms voltage-clamp pulses to +25 mV from a V_h of −40 mV in normal ASW and in ASW containing 100 mM-TEA. Note block of the outward current in 100 mM-TEA ASW. *B*, tail currents following the pulses given in *A*. Note different time scale.

Accumulation of external K^+ would cause a transient shift in E_K and a transient inward shift in the current required to hold the membrane at a given potential. The slow decay of an inward current generated by such a mechanism might account for the phase II tail current. The increase in external K^+ should be proportional to the K^+ efflux during the depolarizing pulse. Therefore, agents which reduce the K^+ current during the pulse should reduce K^+ accumulation. Fig. 4*A* demonstrates that the large outward K^+ current which is activated by voltage-clamp pulses in normal ASW is largely blocked by the addition of 100 mM-TEA to the bathing medium. However, the phase II tail current which follows the pulse is only slightly reduced by TEA (Fig. 4*B*); in three l.u.q.b. cells the phase II tail current was reduced by 12–20% following the addition of 100 mM-TEA. In each case the net current generated by 60–90 mV depolarizing pulses (10–30 ms duration) remained inward

throughout the pulse in the presence of TEA. The small decrease in the net phase II tail current is probably due to a slight increase in the opposing phase III tail current which occurs in TEA-containing ASW (Kramer & Zucker, 1985). Thus, as is the case in *Tritonia* bursting neurones (Thompson, 1976), the phase II tail current is not blocked by eliminating the K^+ current during the pulse, and is therefore not due to external K^+ accumulation.

Ionic specificity of the phase II tail current. The contribution of various ion species in carrying all or part of the phase II tail current was investigated by varying the concentrations of external ions. The contribution of Ca^{2+} as a current-carrying ion could not be ascertained because the phase II tail current is activated by Ca^{2+} influx (Fig. 2), and therefore a reduction of the phase II tail current following removal of external Ca^{2+} could represent either the lack of its activation, or a reduction of a component of the current carried by Ca^{2+}. The inward tail current in *Tritonia* neurones is reduced by about 50 % if external Na^+ is replaced with sucrose or Tris, suggesting that part of the current is carried by Na^+ (Thompson, 1976). In *Aplysia* l.u.q.b. cells, the phase II tail current elicited at a V_h of -60 mV was reduced by $60{\cdot}1 \pm 14{\cdot}3$ % ($n = 8$) following replacement of external Na^+ with TMA^+. The degree of reduction of the phase II tail current in TMA^+-substituted ASW was quite variable, ranging from 46–74 %. This effect was largely reversible; the phase II tail current returned to $95 \pm 1{\cdot}3$ % ($n = 4$) of its initial amplitude upon re-addition of Na^+ to the

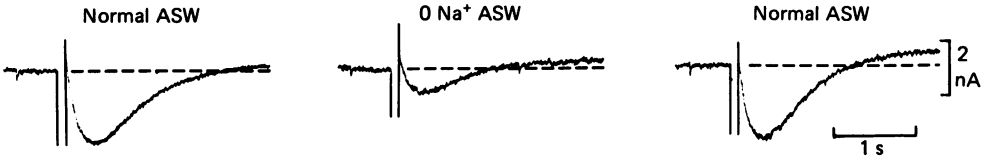

Fig. 5. Effect of external Na^+ on the phase II tail current elicited by 20 ms pulses to +20 mV from a V_h of -60 mV. The tail currents were elicited in normal ASW, 10 min after replacement of external Na^+ with TMA^+, and 10 min after returning to normal ASW.

bathing medium. In two cells, external Na^+ was substituted with sucrose. The phase II tail current in these cells was reduced by 60 % and 70 %, and returned to 84–96 % of its initial value upon re-addition of Na^+. As noted above, in some l.u.q.b. cells substitution of Li^+ for Na^+ caused little or no reduction in the tail current, suggesting that Li^+ can permeate the channels which underlie phase II, similar to the high permeability of Li^+ through voltage-dependent Na^+ channels (Adams & Gage, 1979).

Substitution of 490 mM (79 %) of the external Cl^- with methylsulphate ions had little effect on the phase II tail current. The effect of the Cl^- substitution ranged from an increase in the phase II current of 9 % to a decrease of 5 % in three cells. Changes of the external K^+ concentration caused changes in the reversal potential and amplitude of phase I tail current (see Kramer & Zucker, 1985) which interfered with measurement of the phase II tail current. Therefore, the possible contribution of K^+ as a current carrier was not determined.

Voltage-dependent persistent Ca^{2+} current

Bursting pace-maker neurones exhibit a persistent inward current which underlies the region of negative slope ('negative resistance region') in the pace-maker potential

range of the steady-state I–V curve (Eckert & Lux, 1976).The pace-maker range is the range of voltage through which the membrane potential can slowly oscillate during bursting pace-maker activity (i.e. −50 to −30 mV). The persistent inward current can be most easily during small (e.g. 10 mV) depolarizing pulses from within the pace-maker range. A portion of the persistent inward current exhibits slow activation and deactivation kinetics (Eckert & Lux, 1976; Kramer & Zucker, 1985); thus the phase II tail current could conceivably be due to the slow decay of this current following a large depolarizing pulse.

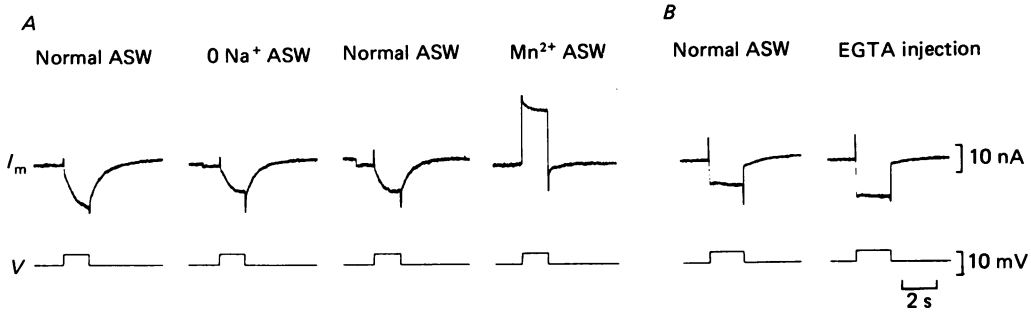

Fig. 6. Voltage-dependent persistent inward current, elicited by 2 s pulses from a V_h of −40 mV to a V_t of −35 mV. *A*, current traces (from left to right) obtained in normal ASW, 10 min after replacement of Na^+ with TMA^+, 10 min after returning to normal ASW, and 15 min after replacement of Ca^{2+} with Mn^{2+}. *B*, persistent inward current, in another l.u.q.b. cell, before (left) and after (right) a 4 min, 400 nA injection of EGTA.

Some important characteristics distinguish the persistent inward current from the phase II tail current. The phase II tail current of l.u.q.b. cells is reversibly reduced by about 60% by substitution of external Na^+ with TMA^+ (Fig. 5). In contrast, equimolar substitution of external Na^+ with TMA^+ caused a decrease in the persistent inward current of only $18{\cdot}2 \pm 2{\cdot}6$% ($n = 4$) (Fig. 6*A*). Upon re-addition of Na^+, the persistent inward current increased by only $8{\cdot}3 \pm 4{\cdot}5$% ($n = 4$). Thus, unlike the phase II tail current, the decrease in the persistent inward current which occurs upon Na^+ substitution is small, and largely irreversible. Therefore, as in *Helix* bursting neurones (Eckert & Lux, 1976), it is unlikely that Na^+ carries any of the persistent inward current in l.u.q.b. cells, although external Na^+ seems to be necessary for its maintenance at normal levels.

The persistent inward current of l.u.q.b. cells, like the phase II tail current, is reversibly blocked by substitution of external Ca^{2+} with Mn^{2+} (Fig. 6) or Co^{2+}. Substitution of external Ca^{2+} with Ba^{2+}, which permeate well through Ca^{2+} channels (for review see Hagiwara & Byerly, 1981), but which only weakly mediate Ca^{2+}-dependent ionic processes (Gorman & Hermann, 1979; Eckert & Tillotson, 1981), causes an increase in the persistent inward current (Eckert & Lux, 1976). Substitution of Ba^{2+} for Ca^{2+}, however, caused a decrease in the phase II tail current of 10–25% in three cells tested (data not shown), as expected for a Ca^{2+}-activated current. Finally, unlike the phase II tail current (Fig. 2*A*2), the persistent inward current was not blocked, but actually increased by $40{\cdot}5 \pm 6{\cdot}1$% ($n = 4$) following intracellular injection of EGTA (Fig. 6*B*). This increase of the persistent inward current is

probably due to the removal of steady-state Ca^{2+}-dependent inactivation of the current by EGTA (Kramer & Zucker, 1985). Another possibility is that the EGTA eliminates a steady-state outward current (i.e. $I_{K(Ca)}$); this does not seem to be the case because we have observed the effect in the presence of 50 mM-TEA, an effective blocker of $I_{K(Ca)}$ (Hermann & Gorman, 1979; Kramer & Zucker, 1985).

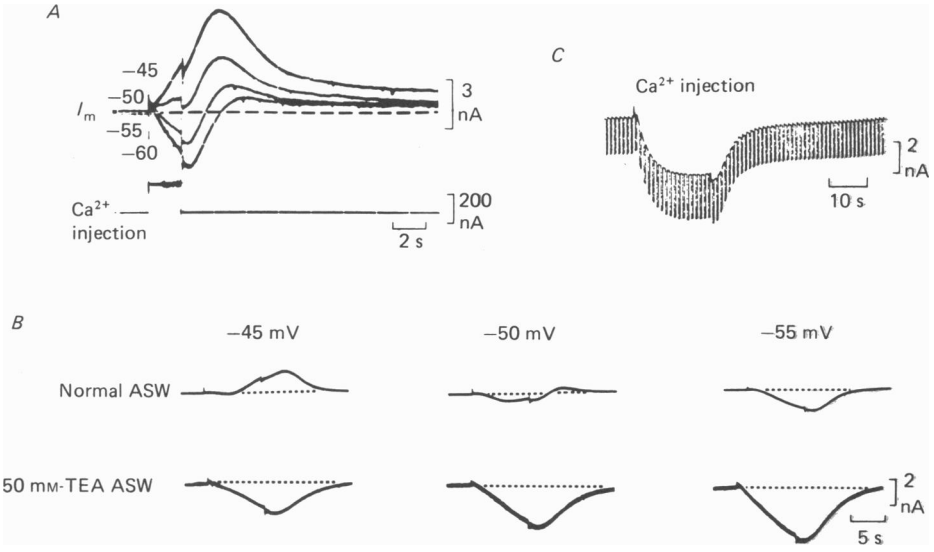

Fig. 7. Ca^{2+}-elicited inward current. *A*, superimposed currents (above) elicited by 2 s, 200 nA injections of Ca^{2+} into a voltage-clamped l.u.q.b. cell at various V_h. The steady-state holding current, at each value of V_h, was defined as zero before the Ca^{2+} injection. The V_h (mV) is noted at the left of each trace. Ca^{2+} injection current monitor is shown below. *B*, currents elicited by 8 s, 200 nA Ca^{2+} injections at three different values of V_h in normal ASW and 50 mM-TEA ASW. The value of V_h (in mV) is noted above each pair of traces. Sharp current deflexions mark the onset and offset of the Ca^{2+} injections. *C*, steady-state conductance increase during the Ca^{2+}-elicited inward current. Current deflexions due to repetitive (about 1 Hz) 200 ms voltage pulses to −65 mV from a V_h of −60 mV. Note the increase (about 22 %) in the amplitude of current deflexions at the peak of the inward current, which was elicited by a 20 s, 200 nA injection of Ca^{2+}. The experiment was done in 50 mM-TEA ASW.

Inward current elicited by Ca^{2+} injection

Since the phase II tail current seems to be activated by Ca^{2+}, an attempt was made to detect a Ca^{2+}-activated inward current during intracellular iontophoretic injections of Ca^{2+}. In both l.u.q.b. cells and R15 cells, Ca^{2+} injection often elicited an inward–outward biphasic current at a V_h of −50 to −60 mV, while at more negative V_h the net current remained inward throughout the response, and at more positive V_h the net current remained outward (Fig. 7*A*). A similar biphasic Ca^{2+}-elicited current has been found in *Helix* bursting neurones (Hofmeier & Lux, 1981). In our experiments, the inward current component was elicited most reliably if the Ca^{2+}-injection electrode was positioned close (i.e. within 50 μm) to the inner surface of the cell membrane, and if an iontophoretic injection current of less than 300 nA

was used. In order to observe the Ca^{2+}-elicited inward current in isolation, we used 50 mM-TEA to block the outward component ($I_{K(Ca)}$) effectively (Hermann & Gorman, 1979; Kramer & Zucker, 1985). The inward current elicited in TEA increases with hyperpolarization (Fig. 7*B*) and is associated with an increase in the membrane conductance, as indicated by an increase in amplitude of current deflexions which were generated by repetitive, 5 mV hyperpolarizing voltage steps (Fig. 7*C*). The conductance measurement was made at a V_h (−60 mV) at which the steady-state *I–V* curve exhibits a nearly linear slope (Kramer & Zucker, 1985) in order to minimize effects of voltage-dependent conductances. Fig. 8 shows the *I–V* relationship of the Ca^{2+}-activated inward current from an l.u.q.b. cell. In this example, the Ca^{2+}-elicited

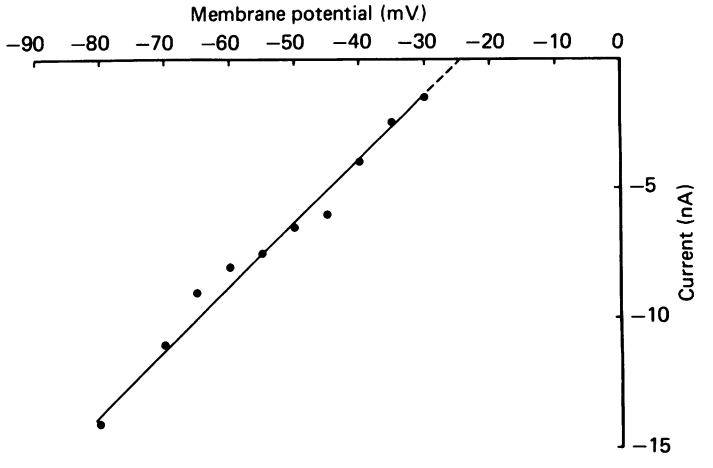

Fig. 8. Current–voltage relation of the peak Ca^{2+}-elicited inward current. Currents were elicited by 4 s, 200 nA injections of Ca^{2+} at different V_h. Dashed line shows extrapolation to the reversal potential of about −24 mV. The bathing solution was 50 mM-TEA ASW.

current had a nearly linear relationship with V_h, with an extrapolated reversal potential between −20 and −30 mV. The linearity of the *I–V* curve varied in different cells; sometimes the inward current began to level out at hyperpolarized potentals (e.g. see *I–V* curves in Fig. 10). The extrapolated reversal potential varied from −5 to −32 mV in different l.u.q.b. cells, with an average value of -22 ± 2 mV ($n = 16$). The Ca^{2+}-elicited inward current component in cell R15 has similar characteristics; all of the results illustrated here, however, were obtained from l.u.q.b. cells.

The Ca^{2+}-elicited inward current always precedes the outwardly directed $I_{K(Ca)}$ during Ca^{2+} injections in normal ASW. The Ca^{2+}-sensitivity of the inward current did not appear to be markedly different from that of the outward current, because we could never activate the Ca^{2+}-activated inward current in isolation from a later, outward component, even if small (< 80 nA) currents were used for injecting Ca^{2+}. The inward–outward sequence of currents during a Ca^{2+} injection might be explained by a difference in the stoicheiometry of the Ca^{2+}-dependent activation of the two currents. The time courses of both the Ca^{2+}-activated inward current and the TEA-blocked outward current during a Ca^{2+} injection are shown in Fig. 9. The two

time courses were obtained from the records of Ca^{2+}-elicited currents in cells held at −45 mV, shown in Fig. 7*B*; the TEA-blocked current was measured by subtracting the current obtained in TEA from the current obtained in normal ASW. If it is assumed that the intracellular Ca^{2+} concentration rises steadily during the course of a Ca^{2+} injection, then the two currents should rise proportionally during an injection if the two species of channels are each activated by the same number of Ca^{2+} ions. However, the Ca^{2+}-activated inward current activates linearly, whereas the TEA-blocked component accelerates during a Ca^{2+} injection, suggesting that more Ca^{2+} ions are necessary for the activation of the TEA-sensitive channels.

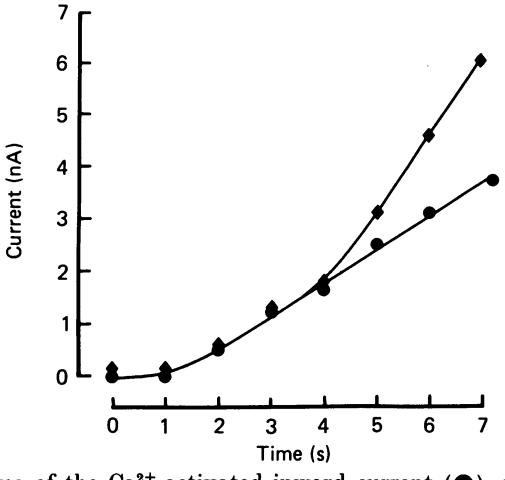

Fig. 9. Time course of the Ca^{2+}-activated inward current (●), and the TEA-sensitive Ca^{2+}-activated current (◆) during an 8 s Ca^{2+} injection. Both components of Ca^{2+}-activated current were obtained from records of currents elicited by Ca^{2+} injections at a V_h of −45 mV in normal ASW and 50 mM-TEA ASW, shown in Fig. 7*B*. The TEA-sensitive component was obtained by graphically subtracting the record obtained in 50 mM-TEA ASW from that obtained in normal ASW.

Ionic specificity of Ca^{2+}-activated inward current

The extracellular concentration of various ions was altered in an attempt to identify the ion species which carry the Ca^{2+}-elicited inward current. All of the bathing solutions used in such experiments contained 50 mM-TEA, in order to block $I_{K(Ca)}$. We did not attempt a quantitative estimate of the relative permeabilities (i.e. permeability ratios) of different ions through the Ca^{2+}-activated channels, because of the high variability of the effectiveness of Ca^{2+} injections. The time course and the maximum amplitude of the inward current often varied from one Ca^{2+} injection to the next, and declined with repeated injection. In addition, changing the bathing solution sometimes caused large changes in the inward current, even if there were no changes in ionic concentrations. It may be that the critical position of the Ca^{2+}-injection electrode with respect to the membrane had changed in those instances.

Substitution of external Na^+ with TMA^+ caused a reduction of the Ca^{2+}-activated inward current (Fig. 10*A*). The Ca^{2+}-dependent conductance change, obtained from the average slope of the *I–V* curve of the inward current between −40 and −60 mV, exhibited a decrease of 14·4 ± 7·0 % (n = 5) and a hyperpolarizing shift in the reversal

potential of 10 ± 6 mV ($n = 5$) following removal of Na^+. An example of the effect of Na^+ removal is shown in Fig. 10*B*. Replacement of external Ca^{2+} with Co^{2+}, resulted in an even smaller decrease in the conductance of $8{\cdot}9 \pm 6{\cdot}7$ % ($n = 5$) and a hyperpolarizing shift of the reversal potential of only 1 ± 3 mV ($n = 5$). An example of the effect of Ca^{2+} removal is shown in Fig. 10*C*. The conductance and the reversal potential exhibited the greatest decrease in a solution in which the Na^+ was replaced with either TMA^+ or sucrose, the Ca^{2+} was replaced with Co^{2+}, Mg^{2+} or Mn^{2+}, and 2 mM-EGTA was added to insure complete removal of external Ca^{2+} (Fig. 10*D*). In

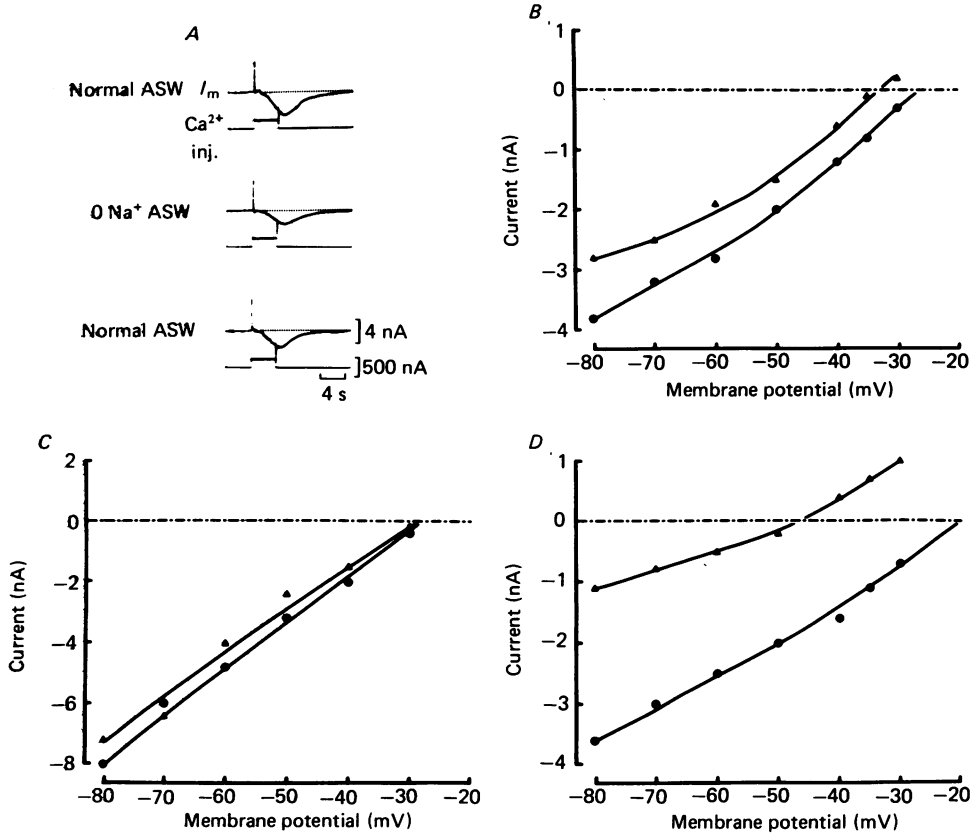

Fig. 10. Effects of ion substitution on the Ca^{2+}-elicited inward current. *A*, currents (above) resulting from 4 s, 200 nA injections of Ca^{2+}, and records of the Ca^{2+}-injection monitor (below). Ca^{2+}-elicited current was obtained in normal ASW, 15 min after replacement of Na^+ with TMA^+, and 15 min after return to normal ASW. *B–D*, current–voltage relations of peak Ca^{2+}-elicited inward current in normal ASW (●), and in 0 Na^+, TMA^+-substituted ASW (▲, *B*); 0 Ca^{2+}, Co^{2+}-substituted ASW (▲, *C*); 0 Na^+, TMA^+-substituted, 0 Ca^{2+}, Mg^{2+}-substituted ASW with 2 mM-EGTA (▲, *D*). In each case, the currents were elicited as in *A*, and the currents in the experimental solution were measured at least 15 min after the bathing solutions were changed. All of the bathing solutions contained 50 mM-TEA.

these solutions the conductance decreased by $38{\cdot}8 \pm 6{\cdot}2$ % ($n = 4$) and the reversal potential shifted in the hyperpolarizing direction by 20 ± 5 mV ($n = 4$). The reversal potential of the Ca^{2+}-elicited current remained between -20 and -30 mV despite changes in the external K^+ concentration from 10 to 1 mM, or from 10 to 40 mM. Changes in the external pH between 6·8 and 8·3 ($n = 4$) also had little effect on the

reversal potential, although the pH change caused a 5–60% decrease in the Ca^{2+}-activated conductance. Replacement of 490 mM (79%) of the external Cl^- with methylsulphate ions resulted in a 0–5% change in the Ca^{2+}-activated conductance and a shift in the reversal potential of less than ± 5 mV. In addition, an l.u.q.b. cell response to iontophoretically applied acetylcholine, previously attributed to an increased Cl^- conductance (Blankenship, Wachtel & Kandel, 1971), exhibited a stable reversal potential of about -55 mV, indicating that E_{Cl} is about 30 mV more hyperpolarized than the reversal potential of the Ca^{2+}-activated inward current. Addition of 50 μM-TTX had no apparent effect on the Ca^{2+}-activated inward current.

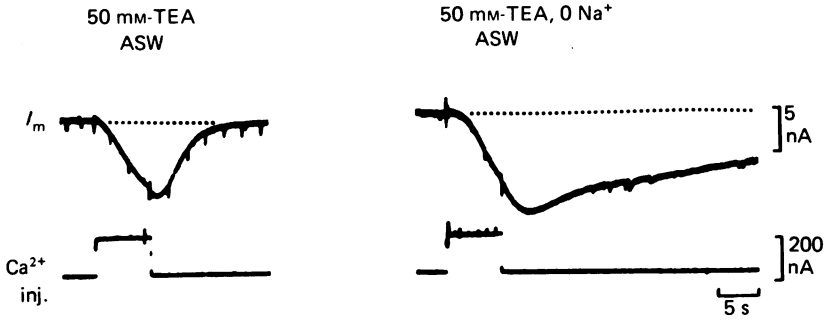

Fig. 11. Currents (above) elicited by 6·7 s, 180 nA injections of Ca^{2+} in normal ASW (left), and 15 min after replacement of external Na^+ with TMA^+ (right). Note increased time-to-peak and prolonged decay of the Ca^{2+}-elicited current. Ca^{2+}-injection current monitor is shown below.

These results suggest that external Na^+, and perhaps Ca^{2+}, contribute to the Ca^{2+}-activated inward current, although the combined contributions of external Na^+ and Ca^{2+} cannot account entirely for the inward current. A complicating factor is that the effective magnitude of the Ca^{2+} injection can increase when external Na^+ is removed. Fig. 11 shows an example of inward currents elicited in Na^+-containing and Na^+-free TMA^+-substituted ASW. Unexpectedly, the peak amplitude of the current was greater after the Na^+ had been replaced with TMA^+. Moreover, the time course of the current was strikingly different after Na^+ removal. In Na^+-containing ASW, the Ca^{2+}-elicited inward current decayed rapidly (within 10 s) after an injection of Ca^{2+}. In Na^+-free ASW, the current persisted for over 2 min after the Ca^{2+} injection. Inward currents activated by subsequent injections of Ca^{2+} progressively diminished, and after six such injections, additional inward current could not be elicited. Such large changes in the time course of the Ca^{2+}-elicited current were more apparent if the Ca^{2+}-injection electrode had been in the cell for more than about 60 min before the removal of external Na^+, although some slowing occurred in cells which had been impaled with the Ca^{2+}-injection electrode as little as 10 min before the removal of Na^+ (e.g. note the slightly slower time-to-peak of the Ca^{2+}-elicited current in Fig. 10*A*).

The time course of the decay of the Ca^{2+}-elicited inward current is probably a reflexion of the time course of the removal of Ca^{2+} from near the region of membrane where the Ca^{2+}-activated cation channels are located. The removal of intracellular Ca^{2+} after an injection is governed by numerous processes (for review, see Requena & Mullins, 1979) including cytoplasmic binding and diffusion of Ca^{2+}, intracellular

sequestration of Ca^{2+} and extrusion of Ca^{2+} across the plasma membrane. It has been demonstrated that extracellular Na^+ is necessary for part of the transport of Ca^{2+} out of squid giant axons (Blaustein & Hodgkin, 1969) and *Aplysia* somata (Satin, 1984). Substitution of Na^+ with TMA^+ may block such a Na^+–Ca^{2+} exchange pump on the *Aplysia* neuronal membrane, thereby inhibiting the removal of Ca^{2+} during and after an injection. Increased accumulation of injected Ca^{2+} in Na^+-free ASW, due to inhibition of the Na^+–Ca^{2+} exchange mechanism, could account for the increased peak Ca^{2+}-elicited inward current, and its slower decay after the injection. The altered time course of Ca^{2+} removal in Na^+-free ASW makes it difficult to accurately estimate the contribution of Na^+ as a charge carrier for the Ca^{2+}-activated inward current. In recognition of these problems, cells whose responses to Ca^{2+} injection were greatly prolonged by Na^+ removal were not included in the analysis of the ionic basis of the Ca^{2+}-elicited inward current.

Voltage dependence of the phase II tail current

As shown in Figs. 8 and 10, the Ca^{2+}-activated inward current declines nearly linearly with membrane potentials between -90 and -35 mV. Therefore, the conductance mechanism activated by Ca^{2+} seems to be largely independent of voltage. If the phase II tail current is due to the slow decline of the same conductance mechanism, then its amplitude should decline linearly when measured at progressively depolarized potentials.

In initial attempts to measure the voltage dependence of the phase II tail current we used a constant pulse potential ($+10$ mV) and varied the holding potential between -65 and -45 mV. Surprisingly, the peak phase II tail current grew larger, rather than smaller, with depolarization within this range (four cells). Similar results have been reported in cell R15 (Lewis, 1984).

This result is partly due to the effects of transient outward K^+ current, I_A (Connor & Stevens, 1971). I_A is inactivated at depolarized holding potentials. At a hyperpolarized holding potential (-65 mV), the phase II tail current is partly obscured by the relaxation of I_A after the pulse, while there is much less contamination at -45 mV. When I_A is blocked by addition of 8 mM-4-aminopyridine (Thompson, 1977), the phase II tail current no longer appeared to increase with depolarization. Instead, its amplitude seemed nearly independent of the holding potential. It still did not decline with depolarization as expected.

We believe that another effect interfering with the measurement of phase II tail current is the contribution of voltage-gated currents arising from the imperfectly voltage-clamped axon stump. More depolarized holding potentials may facilitate the development of regenerative inward currents in the axon, which may contribute to the amplitude of the phase II tail current. Adams & Levitan (1985) have found this to be a particularly serious problem in cell R15.

To counter this problem, we use a two-pulse paradigm, in which a pulse to $+15$ mV (V_1) was followed by a post-pulse to various potentials (V_2) (Fig. 12*A*). The currents generated during V_2 are the result of two factors. First, the V_2 pulse elicits both a leak current and time- and voltage-dependent ionic currents. Secondly, the V_1 pulse initiates the characteristic tail currents, whose magnitudes depend on V_2. In order to isolate the tail currents, the current elicited during a pulse to V_2 alone was subtracted from the current generated during a V_1, V_2 pulse sequence.

Next, we had to estimate the phase II tail current amplitude, in the presence of phase I and phase III components. We reduced phase I currents by eliminating I_A currents with 8 mM-4-aminopyridine and $I_{K(Ca)}$ currents with 50 mM-TEA. Phase III currents decay so little in the time between the V_1 pulse and the phase II peak that they can easily be extrapolated to the phase II peak and subtracted.

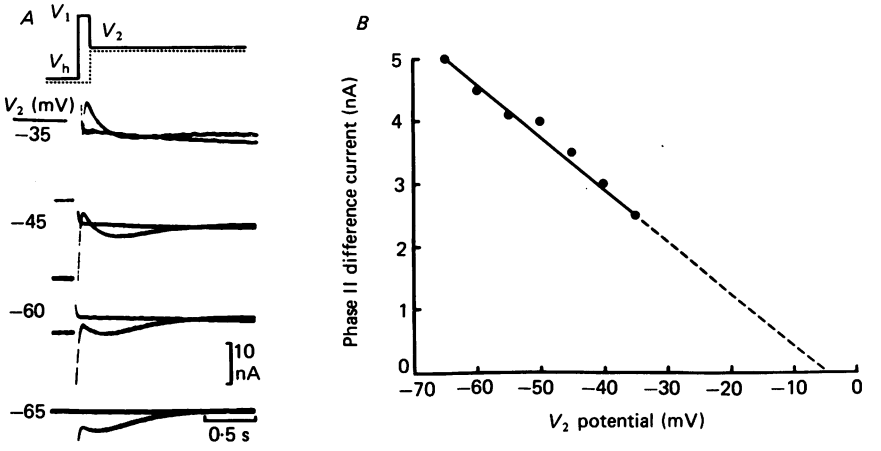

Fig. 12. Voltage dependence of the phase II tail current. *A*, pulse paradigm used to determine the voltage dependence of the phase II tail current. Currents elicited by steps to V_2 (dotted line) are presented with the currents elicited by V_1, V_2 pulse sequences (continuous line). *B*, relation between the peak phase II tail current and the V_2 potential. The phase III tail current, estimated at 2 s after the V_1 pulse, was subtracted from the phase II tail current peak, as described in the text. Bathing solution was 50 mM-TEA ASW, including 8 mM-4-aminopyridine and 50 μM-TTX.

The apparent voltage sensitivity of the phase II tail current measured with the V_1, V_2 pulse paradigm varied depending upon the V_h used. If the V_h was set to −40 mV, then the phase II tail current amplitude decreased slightly as the V_2 potential became more hyperpolarized (not illustrated). This result again suggests that relatively depolarized holding potentials favour the development of regenerative action currents in the axon stump. In preliminary experiments, we have performed intra-axonal recordings 300 μm from the soma and have found regenerative depolarizations which correlate with extra inward current recorded from the voltage-clamped soma. When the axon is hyperpolarized, or when a more hyperpolarized soma holding potential is used, these regenerative axonal depolarizations and their associated inward currents in the soma are abolished (R. H. Kramer, unpublished observations).

We thus used a relatively hyperpolarized holding potential (−65 mV) and added TTX (50 μM) to block voltage-dependent Na^+ current. Using all these precautions, we found that in three cells, the phase II tail current amplitude decreased as the V_2 potential became more depolarized, as expected for a current with a reversal potential more positive than the resting potential. Results from one cell are presented in Fig. 12.

DISCUSSION

The evidence presented here indicates that the phase II tail current is due to the slow relaxation of a Ca^{2+}-activated inward current. It has several characteristics in common with a much more widely studied Ca^{2+}-activated current, $I_{K(Ca)}$. The phase II tail is activated maximally by depolarizing pulses which promote Ca^{2+} entry, and suppressed by large depolarizing pulses which approach E_{Ca}, similar to the behaviour of $I_{K(Ca)}$ (Meech & Standen, 1975). In addition, the phase II tail current is blocked by the Ca^{2+}-channel blockers Co^{2+} and Mn^{2+}, and it is eliminated by internal EGTA. Perhaps most importantly, just as a K^+ current can be activated directly by intracellular injection of Ca^{2+} (Gorman & Hermann, 1979), an inward current with many characteristics in common to the phase II current is also activated by Ca^{2+} injection.

We have excluded a number of mechanisms which could underlie the generation of the phase II tail current. The tail current is not a result of uncontrolled TTX-sensitive Na^+ spikes in the axon stump, although there is a possibility that a portion of the phase II tail current is contributed by Ca^{2+}-dependent regenerative responses in unclamped regions of the cell. The tail current is not a result of activation of an electrogenic Na^+–Ca^{2+} exchange pump; it is not blocked by substitution of Na^+ with Li^+. The tail current is not due to activation of an electrogenic Na^+–K^+ exchange pump; it is not blocked by ouabain. The tail current is not dependent upon the magnitude of the K^+ current in the preceding depolarizing pulse; therefore it is not due to the effects of K^+ accumulation outside the cell. One remaining explanation is that the phase II tail current is due to a Ca^{2+}-dependent change in the membrane conductance to one or more ions. Using small voltage pulses, we have measured an increase in the steady-state membrane conductance during the phase II tail current (R. H. Kramer & R. S. Zucker, unpublished observations). However, these measurements are not specific to the phase II tail current because there are other conductance changes (e.g. the Ca^{2+}-dependent K^+ conductance: Kramer & Zucker, 1985) which overlap with the phase II tail current. Moreover, we have not been able to measure possible instantaneous conductance changes which may be associated with the slow tail currents in l.u.q.b. cells. These conductance changes should be a small fraction of the resting conductance, and may be undetectable (see Kramer & Zucker, 1985).

The Ca^{2+}-elicited inward current of molluscan bursting neurones has been largely overlooked (but see Hofmeier & Lux, 1981) because it is usually obscured by $I_{K(Ca)}$. In the presence of external TEA, however, the current is quite clear. The Ca^{2+}-activated current has an extrapolated reversal potential which falls between -5 and -30 mV, and the underlying conductance seems to be independent of membrane potential. The reversal potential of the Ca^{2+}-activated inward current could be underestimated because of contamination with an opposing current, such as an outward current due to the Ca^{2+}-dependent inactivation of a resting voltage-dependent inward Ca^{2+} current (Kramer & Zucker, 1985). This does not seem likely, because the reversal potential of the Ca^{2+}-elicited current is affected little by substitution of external Ca^{2+} with Ca^{2+}-channel blockers, such as Co^{2+}.

The reversal potential of the Ca^{2+}-elicited inward current does not correspond to the expected equilibrium potential of any single ion species present, except perhaps

H^+ or Cl^-. Changes in the external pH between 8·3 and 6·7, however, do not affect the reversal potential. Nearly complete removal of external Cl^- also does not change the reversal potential. Thus, it is likely that the Ca^{2+}-elicited inward current is not carried by a single ion species, but is due to a conductance increase to a combination of different ions. The results of ion substitution experiments (Fig. 10) support this hypothesis. The Ca^{2+}-elicited current is not carried exclusively by Na^+; it is not completely blocked by the replacement of Na^+ with TMA^+ or with sucrose. The current is not carried exclusively by Ca^{2+}; it is only slightly reduced by replacement of external Ca^{2+} with Co^{2+} or Mg^{2+}. The current is not completely blocked by the complete removal of external Na^+ and Ca^{2+}, although the conductance decreases by about 40%, and the reversal potential shifts by about −20 mV. The remaining Ca^{2+}-elicited current, and the hyperpolarizing shift in the reversal potential, suggest that another ion species, probably K^+, can permeate the Ca^{2+}-activated channels. These channels may also be weakly permeant to the TMA^+ and divalent cations used to replace Na^+ and Ca^{2+}.

The reversal potential of the Ca^{2+}-activated current is consistent with a relatively non-specific increase in permeability to cations. Considering only monovalent cations, and assuming an internal Na^+ activity of 23 mM (Brown & Kunze, 1974) and an internal K^+ activity of 155 mM (Coyer, Halsey & Strong, 1983), the ratio of Na^+/K^+ permeability calculated from the Goldman equation is 0·18 for a current with a reversal potential of −22 mV. The lack of a large effect of changing the external K^+ concentration on the reversal potential of the Ca^{2+}-activated inward current is consistent with the calculated permeability ratio. Changing the K^+ concentration from 10 to 1 mM, or from 10 to 40 mM, should shift the reversal potential only −2·5 mV or +7·0 mV respectively. Changing the K^+ concentration in a medium which contains no Na^+ and Ca^{2+} should shift the reversal potential substantially, but in such a medium the remaining Ca^{2+}-activated current is so small (see Fig. 10*D*) that the effects of changing external K^+ are impossible to discern against the background of variable responses to repeated Ca^{2+} injections. Taken together, the results indicate that the Ca^{2+}-activated conductance seems to be due to a relatively non-selective increase in permeability to a number of cations, primarily Na^+, K^+ and Ca^{2+}.

The exact permeability ratios of the various ions which underlie the Ca^{2+}-elicited inward current of l.u.q.b. neurones are difficult to determine. The effectiveness of Ca^{2+} injections varies under different conditions, such as position of the Ca^{2+}-injection electrode, number and size of prior injections, and effectiveness of Ca^{2+} removal by metabolic and exchange pumps. In particular, the contribution of Na^+ in carrying the Ca^{2+}-elicited inward current may be underestimated because of blockade of the Na^+–Ca^{2+} exchange mechanism following the removal of external Na^+ (see Fig. 11). In addition, the contribution of Ca^{2+} may be underestimated due to difficulty in completely removing Ca^{2+} from extracellular spaces surrounding molluscan neurones (see Akaike *et al.* 1983). The sum of the independent contributions of Na^+ and Ca^{2+} to the Ca^{2+}-elicited inward current, as judged by the reduction of the conductance and shifting of the reversal potential when each of the ions are removed from the external medium, does not seem to equal the conductance change and reversal potential shift due to the simultaneous removal of Na^+ and Ca^{2+}. This may indicate that the relative permeabilities of the two ions depends upon the external concen-

tration of the two ions. Such a change in ionic specificity has been reported to occur in Ca^{2+} channels: there is a dramatic increase in the permeability of Ca^{2+} channels to monovalent cations when external Ca^{2+} is thoroughly removed with EDTA (Kostyuk, Mironov & Shuba, 1983).

Non-selective, Ca^{2+}-activated cation channels have been found in a variety of cell types including cultured cardiac muscle fibres (Colquhoun, Neher, Reuter & Stevens, 1981), neuroblastoma cells (Yellen, 1982) and pancreatic acinar cells (Maruyama & Peterson, 1982). In each case, the mean open time of the channel was found to be dependent on the internal Ca^{2+} concentration and independent of membrane potential. The channels are permeable to both Na^+ and K^+, and impermeable to anions such as Cl^-. Hence the Ca^{2+}-activated, non-specific cation channel appears to be quite widespread.

Disparities between the phase II tail current and the Ca^{2+}-elicited current

There are two main disparities between the behaviour of the phase II tail current and the behaviour of the inward current elicited by Ca^{2+} injection. First, the phase II tail current seems to be more sensitive to the external Na^+ concentration than is the Ca^{2+}-elicited inward current. Secondly, the voltage-sensitivity of the phase II tail current and the Ca^{2+}-elicited current appear to be different; the Ca^{2+}-elicited inward current grows larger with hyperpolarization and has a reversal potential near -20 mV, whereas the phase II tail current does not necessarily become larger at hyperpolarized V_h.

Contribution of Na^+. Removal of Na^+ from the bathing medium results in reduction of the phase II tail current by about 60 % (Fig. 5), while the reversal potential of the Ca^{2+}-elicited current shifts by less than -10 mV and the conductance is reduced by only 15 % (Fig. 10). One possible explanation for the great Na^+ sensitivity of the phase II tail current is that Na^+ removal leads to an accumulation of Ca^{2+} inside the cell, due to a block of the Na^+–Ca^{2+} exchange pump. The increase of intracellular Ca^{2+} could result in a partial inactivation of the Ca^{2+} current during the depolarizing pulse (see Eckert & Tillotson, 1981; Plant, Standen & Ward, 1983), leading to a *decrease* of the Ca^{2+}-dependent activation of the phase II tail current. In contrast, a blocked Na^+–Ca^{2+} pump might *enhance* the effect of Ca^{2+} injection. It has been demonstrated that Ca^{2+} extrusion from *Aplysia* neurones is partly dependent upon the presence of external Na^+ (Satin, 1984). The decrease of the persistent inward current upon Na^+ removal in cell R15 (Smith *et al.* 1975) and in the l.u.q.b. cells (Fig. 6) is blocked in cells which have been pre-injected with EGTA (Gorman *et al.* 1982), suggesting that the effects of Na^+ removal are dependent upon the build-up of intracellular Ca^{2+}. The activity of the Na^+–Ca^{2+} exchange pump may be especially important for the long-term regulation of the ambient Ca^{2+} concentration in bursting neurones, because they have a large Ca^{2+} conductance (Gorman & Hermann, 1982), some of which is activated at a membrane potential as low as -50 mV (Kramer & Zucker, 1985). The Na^+–Ca^{2+} exchange mechanism has a low affinity for intracellular Ca^{2+} (DiPolo & Beaugé, 1983); hence its importance in regulating the internal Ca^{2+} concentration is enhanced by a high internal Ca^{2+} level. Thus, the sensitivity of the phase II tail current to removal of external Na^+ may vary with the ambient intracellular Ca^{2+} concentration.

Voltage sensitivity. The voltage dependence of the phase II tail current is strongly influenced by experimental procedure. Only when I_A and $I_{K(Ca)}$ contributions to phase I tail currents are pharmacologically blocked and regenerative axonal currents reduced with TTX and with a hyperpolarized holding potential does the phase II tail current increase with hyperpolarizing and decrease with depolarizing post-pulses. Even then, the extrapolated reversal potential for phase II current is about -5 mV (see Fig. 12), while that of Ca^{2+}-elicited inward current is about -22 mV (Fig. 8). This discrepancy probably arises from the difficulty in estimating phase II amplitudes. Phase II tail current occurs simultaneously with residual phase I tail current, due to voltage-dependent K^+ channels, and phase III tail current, which is also voltage-dependent (Kramer & Zucker, 1985). This precludes accurate estimation of the phase II peak amplitude. Furthermore, we have probably still not succeeded in blocking completely axonal action currents, particularly those due to voltage-dependent Ca^{2+} current. These will increase with depolarization, partially offsetting the reduction in the driving force of the phase II tail current generated in the soma. Thus, despite the pharmacological and procedural precautions taken in Fig. 12, we do not feel that we have found a method by which to accurately and unambiguously measure the voltage dependence of phase II current.

Role of the Ca^{2+}-activated inward current in bursting pace-maker activity

The Ca^{2+}-dependent ionic conductance which underlies the phase II tail current is one of two conductances which contribute to the depolarizing phase of bursting pace-maker activity. It is distinct from the persistent Ca^{2+} conductance, which is voltage-dependent and inactivated by intracellular Ca^{2+} (Kramer & Zucker, 1985). The relative contributions of the two conductances in generating the negative resistance characteristic, seen in the pace-maker potential region of the steady-state I–V curve, are unknown, although injection of bursting cells with EGTA, which blocks the phase II tail current, leads to an increase rather than a decrease in the amplitude of the negative resistance characteristic (Gorman *et al.* 1982). In untreated cells, the sensitivity of the negative resistance to external Na^+ in addition to Ca^{2+} (Smith *et al.* 1975) may be due, in part, to a contribution from the phase II current. It is not known whether the phase II current is necessary for maintenance of membrane potential oscillations in bursting neurones. The phase II tail current underlies the generation of d.a.p.s in l.u.q.b. cells (Fig. 1) and in cell R15 (Lewis, 1984; Adams, 1985). A similar current may underlie Ca^{2+}-dependent d.a.p.s in crab muscle fibres (Suarez-Kurtz, 1979) and mammalian cardiac fibres (Kass, Lederer, Tsien & Weingart, 1978). The d.a.p. of bursting neurones may serve to increase the depolarizing drive during the burst, leading to repetitive firing. A qualitative model of the involvement of the phase II tail current, the persistent Ca^{2+} current, and $I_{K(Ca)}$ in bursting pace-maker activity is presented in the following paper (Kramer & Zucker, 1985).

We are grateful to Russell English and Darrell Dodson for valuable technical assistance, and to Drs William Adams, Irwin Levitan and John Miller for reading the manuscript. The work was supported by NIH grant NS 15114.

REFERENCES

ADAMS, D. J. & GAGE, P. W. (1979). Ionic currents in response to membrane depolarization in an *Aplysia* neurone. *Journal of Physiology* **289**, 115–141.

ADAMS, W. B. (1985). Slow depolarizing and hyperpolarizing currents which mediate bursting in *Aplysia* neurone R15. *Journal of Physiology* **360**, 51–68.

ADAMS, W. B. & LEVITAN, I. B. (1985). Voltage and ion dependences of the slow currents which mediate bursting in *Aplysia* neurone R15. *Journal of Physiology* **360**, 69–93.

AKAIKE, N., BROWN, A. M., DAHL, G., HIGASHI, H., ISENBERG, G., TSUDA, Y. & YATANI, A. (1983). Voltage-dependent activation of potassium current in *Helix* neurones by endogenous cellular calcium. *Journal of Physiology* **334**, 309–324.

ALVING, B. O. (1968). Spontaneous activity in isolated somata of *Aplysia* pacemaker neurons. *Journal of General Physiology* **51**, 29–45.

ANDREW, R. D. & DUDEK, F. E. (1983). Burst discharge in mammalian neuroendocrine cells involves an intrinsic regenerative mechanism. *Science* **221**, 1050–1052.

BLANKENSHIP, J. E., WACHTEL, H. & KANDEL, E. R. (1971). Ionic mechanisms of excitatory, inhibitory, and dual synaptic actions mediated by an identified interneuron in abdominal ganglion of *Aplysia*. *Journal of Neurophysiology* **34**, 76–92.

BLAUSTEIN, M. P. & HODGKIN, A. L. (1969). The effect of cyanide on the efflux of calcium from squid axons. *Journal of Physiology* **200**, 497–527.

BREHM, P. & ECKERT, R. (1978). Calcium entry leads to inactivation of calcium channel in *Paramecium*. *Science* **202**, 1203–1206.

BROWN, A. M. & KUNZE, D. L. (1974). Ionic activities in identifiable *Aplysia* neurons. In *Ion-Selective Microelectrodes*, ed. BERMAN, H. J. & HEBERT, N. C., pp. 57–69. New York: Plenum Press.

CALABRESE, R. L. (1979). The roles of endogenous membrane properties and synaptic interaction in generating the heartbeat rhythm of the leech *Hirudo medicinalis*. *Journal of Experimental Biology* **82**, 163–176.

CARNEVALE, N. T. & WACHTEL, H. (1980). Two reciprocating current components underlying slow oscillations in Aplysia bursting neurons. *Brain Research Reviews* **2**, 45–68.

COLQUHOUN, D., NEHER, E., REUTER, H. & STEVENS, C. F. (1981). Inward current channels activated by intracellular Ca in cultured cardiac cells. *Nature* **294**, 752–754.

CONNOR, J. A. & STEVENS, C. F. (1971). Voltage clamp studies of a transient outward membrane current in gastropod neural somata. *Journal of Physiology* **213**, 21–30.

COYER, P. E., HALSEY JR, J. H. & STRONG, E. R. (1983). Reversible changes in the intracellular potassium ion activities and membrane potentials of *Aplysia* L_2–L_6 neurones in response to normoxia and hypoxia. *Journal of Experimental Biology* **102**, 79–92.

DIPOLO, R. & BEAUGÉ, L. (1983). The calcium pump and sodium–calcium exchange in squid axons. *Annual Review of Physiology* **45**, 313–324.

EATON, D. C. (1972). Potassium ion accumulation near a pace-making cell of *Aplysia*. *Journal of Physiology* **224**, 421–440.

ECKERT, R. & LUX, H. D. (1976). A voltage-sensitive persistent calcium conductance in neuronal somata of *Helix*. *Journal of Physiology* **254**, 129–151.

ECKERT, R. & TILLOTSON, D. (1981). Calcium-mediated inactivation of the calcium conductance in caesium-loaded giant neurones of *Aplysia californica*. *Journal of Physiology* **314**, 265–280.

FRAZIER, W. T., KANDEL, E. R., KUPFERMANN, I., WAZIRI, R. & COGGESHALL, R. E. (1967). Morphological and functional properties of identified neurons in the abdominal ganglion of *Aplysia californica*. *Journal of Neurophysiology* **30**, 1288–1351.

GAHWILER, B. H. & DREIFUSS, J. J. (1979). Phasically firing neurons in long term cultures of the rat hypothalamic supraoptic area: pacemaker and follower cells. *Brain Research* **177**, 95–103.

GAINER, H. (1972). Electrophysiological activity of an endogenously active neurosecretory cell. *Brain Research* **39**, 403–418.

GOLA, M. & SELVERSTON, A. (1981). Ionic requirements for bursting activity in lobster stomatogastric neurons. *Journal of Comparative Physiology* **145**, 191–207.

GORMAN, A. L. F. & HERMANN, A. (1979). Internal effects of divalent cations on potassium permeability in molluscan neurones. *Journal of Physiology* **296**, 393–410.

GORMAN, A. L. F. & HERMANN, A. (1982). Quantitative differences in the currents of bursting and beating pace-maker neurones. *Journal of Physiology* **333**, 681–699.

GORMAN, A. L. F., HERMANN, A. & THOMAS, M. V. (1982). Ionic requirements for membrane oscillations and their dependence on the calcium concentration in a molluscan bursting pace-maker neurone. *Journal of Physiology* **327**, 185–217.

GORMAN, A. L. F. & THOMAS, M. V. (1980*a*). Potassium conductance and internal calcium accumulation in a molluscan neurone. *Journal of Physiology* **308**, 287–313.

GORMAN, A. L. F. & THOMAS, M. V. (1980*b*). Intracellular calcium accumulation during depolarization in a molluscan neurone. *Journal of Physiology* **308**, 259–285.

GRAUBARD, K. (1975). Voltage attenuation within *Aplysia* neurons: the effect of branching pattern. *Brain Research* **88**, 325–332.

HAGIWARA, S. & BYERLY, L. (1981). Calcium channel. *Annual Review of Neuroscience* **4**, 69–125.

HERMANN, A. & GORMAN, A. L. F. (1979). External and internal effects of tetraethylammonium on voltage-dependent and Ca-dependent K^+ currents components in molluscan pacemaker neurons. *Neuroscience Letters* **12**, 87–92.

HOFMEIER, G. & LUX, H. D. (1981). The time course of intracellular free calcium and related electrical effects after injection of $CaCl_2$ into neurons of the snail, *Helix pomatia*. *Pflügers Archiv* **391**, 242–251.

JOHNSTON, D. (1976). Voltage clamp reveals basis for calcium regulation of bursting pacemaker potentials in *Aplysia* neurons. *Brain Research* **107**, 418–423.

KASS, R. S., LEDERER, W. J., TSIEN, R. W. & WEINGART, R. (1978). Role of calcium ions in transient inward currents and aftercontractions induced by strophanthidin in cardiac Purkinje fibres. *Journal of Physiology* **281**, 187–208.

KATZ, B. & MILEDI, R. (1967). A study of synaptic transmission in the absence of nerve impulses. *Journal of Physiology* **192**, 407–436.

KOSTYUK, P. G., MIRONOV, S. L. & SHUBA, YA. M. (1983). Two ion-selecting filters in the calcium channel of the somatic membrane of mollusc neurons. *Journal of Membrane Biology* **76**, 83–93.

KRAMER, R. H. & ZUCKER, R. S. (1985). Calcium-induced inactivation of calcium current causes the inter-burst hyperpolarization of *Aplysia* bursting neurones. *Journal of Physiology* **362**, 131–160.

LEWIS, D. V. (1984). Spike aftercurrents in R15 of *Aplysia*: their relationship to slow inward current and calcium influx. *Journal of Neurophysiology* **51**, 387–403.

LEWIS, D. V., EVANS, G. B. & WILSON, W. A. (1984). Dopamine reduces slow outward current and calcium influx in burst firing neuron R15 of *Aplysia*. *Journal of Neuroscience* **4**, 3014–3020.

MARUYAMA, Y. & PETERSEN, O. H. (1982). Single-channel currents in isolated patches of plasma membrane from basal surface of pancreatic acini. *Nature* **299**, 159–161.

MEECH, R. W. (1978). Calcium-dependent potassium activation in nervous tissues. *Annual Review of Biophysics and Bioengineering* **7**, 1–18.

MEECH, R. W. & STANDEN, N. B. (1975). Potassium activation in *Helix aspersa* neurones under voltage clamp: a component mediated by calcium influx. *Journal of Physiology* **249**, 211–239.

NEHER, E. & LUX, H. D. (1973). Rapid changes of potassium concentration at the outer surface of exposed single neurons during membrane current flow. *Journal of General Physiology* **61**, 385–389

PLANT, T. D., STANDEN, N. B. & WARD, T. A. (1983). The effects of calcium ions and calcium chelators on calcium channel inactivation in *Helix* neurones. *Journal of Physiology* **334**, 189–212.

REQUENA, J. & MULLINS, L. J. (1979). Calcium movement in nerve fibers. *Quarterly Review of Biophysics* **12**, 371–460.

SATIN, L. (1984). Sodium-dependent calcium efflux from single *Aplysia* neurons. *Brain Research* **300**, 392–395.

SMITH, S. J. (1978). The mechanism of bursting pacemaker activity in neurons of the mollusc *Tritonia diomedia*. Ph.D. dissertation, University of Washington, Seattle, WA.

SMITH, S. J. & ZUCKER, R. S. (1980). Aequorin response facilitation and intracellular calcium accumulation in molluscan neurones. *Journal of Physiology* **300**, 167–196.

SMITH JR, T. G., BARKER, J. L. & GAINER, H. (1975). Requirements for bursting pacemaker potential activity in molluscan neurones. *Nature* **253**, 450–452.

SUAREZ-KURTZ, G. (1979). The depolarizing afterpotential of crab muscle fibres. A sodium-dependent process mediated by intracellular calcium. *Journal of Physiology* **286**, 317–329.

TAZAKI, K. & COOKE, I. M. (1979). Isolation and characterization of slow, depolarizing responses of cardiac ganglion neurons in the crab, *Portunus sanguinolentus*. *Journal of Neurophysiology* **42**, 1000–1021.

THOMPSON, S. H. (1976). Membrane currents underlying bursting in molluscan pacemaker neurons. Ph.D. dissertation, University of Washington, Seattle, WA.

THOMPSON, S. H. (1977). Three pharmacologically distinct potassium channels in molluscan neurones. *Journal of Physiology* **265**, 465–488.

THOMPSON, S. H. & SMITH, S. J. (1976). Depolarizing afterpotentials and burst production in molluscan pacemaker neurons. *Journal of Neurophysiology* **39**, 153–157.

TREISTMAN, S. N. (1980). Axonal site for impulse initiation and rhythmogenesis in *Aplysia* pacemaker neurons. *Brain Research* **187**, 201–205.

YELLEN, G. (1982). Single Ca^{2+}-activated nonselective cation channels in neuroblastoma. *Nature* **296**, 357–359.